

Surface waves in a vertically excited circular cylindrical container*

Jian Yong-Jun(菅永军)^{a)b)†}, E Xue-Quan(鄂学全)^{b)},
Zhang Jie(张杰)^{a)c)}, and Meng Jun-Min(孟俊敏)^{a)c)}

^{a)}First Institute of Oceanography, State Oceanic Administration, Qingdao 266061, China

^{b)}Institute of Mechanics, Chinese Academy of Sciences, Beijing 100080, China

^{c)}Key Laboratory of Marine Science and Numerical Modelling, State Ocean Administration, Qingdao 266061, China

(Received 13 November 2003; revised manuscript received 25 May 2004)

The nonlinear free surface amplitude equation, which has been derived from the inviscid fluid by solving the potential equation of water waves with a singular perturbation theory in a vertically oscillating rigid circular cylinder, is investigated successively in the fourth-order Runge–Kutta approach with an equivalent time-step. Computational results include the evolution of the amplitude with time, the characteristics of phase plane determined by the real and imaginary parts of the amplitude, the single-mode selection rules of the surface waves in different forced frequencies, contours of free surface displacement and corresponding three-dimensional evolution of surface waves, etc. In addition, the comparison of the surface wave modes is made between theoretical calculations and experimental measurements, and the results are reasonable although there are some differences in the forced frequency.

Keywords: vertically forced oscillation, nonlinear amplitude equation, phase-plane, surface wave modes

PACC: 0340G, 4754, 5235M, 9530L

1. Introduction

Faraday^[1](1831) put a vessel filled with different fluids on a vertically vibrating plate, and the free surface of the fluid formed various beautiful surface waves. He realized that these surface waves have a frequency equal to a half that of the excitation. However, Faraday could not give an explanation to this phenomenon theoretically. Benjamin & Ursell^[2] (1954) established the linear theory of this problem and derived a so-called Mathieu equation, which governed each surface wave mode and included the effect of surface tension. Skalak & Yarymovych^[3] (1962) and Ockendon & Ockendon^[4] (1973) demonstrated the weakly nonlinear Faraday resonance by using the perturbation expansion method. A review of this subject was given by Miles^[5,6] (1984a, 1993) and Miles & Henderson^[7] (1990). The effect of viscosity was discussed by Kumar & Tuckerman^[8] (1994) and Cerda & Tirapegui^[9] (1998).

Much of the current interest in the Faraday resonance arises from the possibility that it is used as

a system with many degrees of freedom and especially as a pattern forming system (Christiansen *et al*^[10] (1995)). The papers concerning Faraday resonance, which had been published before 1984, dealt with the wave motions with only one spatial mode assumed to be excited. Most of the recent papers are involved with two or more spatial modes that are interacted with each other mainly due to the fact that chaotic motions possibly occur in the process of wave excitation (Ciliberto & Gollub^[11] (1985), Gollub & Meyer^[12] (1983)).

However, the theory of single-mode excitation is not yet complete; it is not involved with some phenomena, such as the structures of the surface wave and its evolution with time. The characteristics of standing waves formed in a circular cylindrical vessel are very different from those in a rectangular vessel. In a circular cylindrical vessel, radial waves expand outwards from center, so they cannot keep their shapes and amplitudes unchanged. E and Gao^[13–15] (1996, 1998) carried out the flowing visualization about free

*Project supported by the National Natural Science Foundation of China (Grant Nos 19772063, 19772068).

†Correspondence author: E-mail: jianyongjun@yahoo.com.cn

surface wave patterns in a circular cylindrical vessel, which was excited by vertical vibration, and obtained many beautiful free surface pattern pictures.

Recently, Jian & E^[16–19] (2003) proposed a mathematical formulation associated with the flowing visualization in Refs.[13–15], from which the second order free surface displacements and their contours were obtained by using the two-time scale singular perturbation expansion. The numerical results indicate that the contours of free surface waves are in good agreement with the above experimental flowing visualization.

In this article, we continue to discuss the characteristics of the amplitude equation derived in Refs.[16–19]. Some comparisons have been made between theoretical calculations and experimental measurements.

2. Amplitude equation and free surface displacement

We consider the surface waves excited by the vertical vibration of a circular cylindrical basin filled with fluid, as shown in Fig.1. We take cylindrical coordinate system (r, θ, z) moving with the vessel, such that the undisturbed free surface is at $z = 0$, and base of the vessel is located at $z = -h < 0$. Here, h denotes the depth of fluid. If the vessel motion is assumed to be at a vertical acceleration \ddot{z}_0 , then the fluid moves relatively to the vessel as if it moves at a gravitational acceleration $(g - \ddot{z}_0)$ in a stationary vessel, where $z_0 = A \cos(2\omega_0 t)$ is the excited displacement of the vessel in the vertical direction, \ddot{z}_0 is the second derivative of z_0 with respect to time t , while A and $2\omega_0$ are the amplitude and angular frequency of the external forcing.

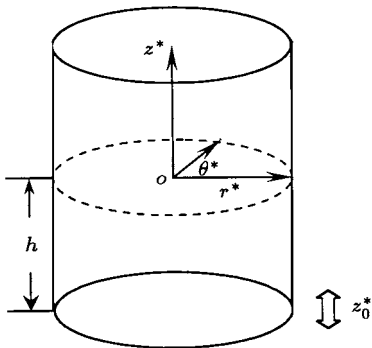


Fig.1. Physical model of the liquid-filled circular cylinder.

In order to resolve this problem, Refs.[16–18] developed the following nonlinear complex amplitude

equation of the free surface displacement:

$$i \frac{dp(\tau)}{d\tau} = M_1 p^2(\tau) \bar{p}(\tau) + M_2 e^{2i\sigma\tau} \bar{p}(\tau), \quad (1)$$

where i is the unit of imaginary number, $p(\tau)$ is called the slowly variable complex amplitude and $\bar{p}(\tau)$ denotes the complex conjugate of $p(\tau)$, τ is a slowly varying time scale, M_1 and M_2 are constants. In addition, we assume that the frequency Ω of the free surface wave is close to half the frequency $2\omega_0$ of forced oscillation, and let $\omega_0 - \Omega = \varepsilon^2\sigma$. The parameter ε quantifies the acceleration due to the vertical oscillation relative to gravity, named as $\varepsilon^2 = 4A\omega_0^2/g$, and is assumed to be much less than unity.

Defining $p_1(\tau)$ and $p_2(\tau)$ as the real and imaginary parts of $p(\tau)$ and dividing Eq.(1) into real and imaginary parts, respectively, yields the following simultaneous nonlinear ordinary differential equations:

$$\begin{aligned} \frac{dp_1(\tau)}{d\tau} &= M_1 p_2(\tau) [p_1^2(\tau) + p_2^2(\tau)] \\ &\quad + M_2 [p_1(\tau) \sin(2\sigma\tau) - p_2(\tau) \cos(2\sigma\tau)], \quad (2) \\ \frac{dp_2(\tau)}{d\tau} &= -M_1 p_1(\tau) [p_1^2(\tau) + p_2^2(\tau)] \\ &\quad - M_2 [p_1(\tau) \cos(2\sigma\tau) + p_2(\tau) \sin(2\sigma\tau)]. \quad (3) \end{aligned}$$

The displacement of free surface can be expressed in the following form:

$$\eta(r, \theta, t, \tau) = \varepsilon\eta_1 + \varepsilon^2\eta_2, \quad (4)$$

where first-order and second-order free surface displacements $\eta_1(r, \theta, t, \tau)$ and $\eta_2(r, \theta, t, \tau)$ have the forms, respectively,

$$\begin{aligned} \eta_1(r, \theta, t, \tau) &= \frac{\lambda}{i\Omega} J_m(\lambda r) \sinh(\lambda h/R) \\ &\quad \times [p(\tau)e^{i\Omega t} - \bar{p}(\tau)e^{-i\Omega t}] \cos m\theta, \quad (5) \\ \eta_2(r, \theta, t, \tau) &= [Y_1(r) + Y_2(r) \cos(2m\theta)] \\ &\quad \times (p^2(\tau)e^{2i\Omega t} + \bar{p}^2(\tau)e^{-2i\Omega t}), \quad (6) \end{aligned}$$

where $\lambda = \lambda_{mn}$ are the positive real roots of $dJ_m(\lambda_{mn}r)/dr|_{r=1} = 0$, $J_m(r)$ is the m th order Bessel function of first kind, R is radius of the vessel, $Y_1(r)$ and $Y_2(r)$ are the functions of the variable r .

3. The characters of the amplitude equation

The amplitude equations (2) and (3) can be solved in the fourth-order Runge–Kutta approach with an equivalent time-step, and the initial amplitude is chosen to be approximate to the wave height of free surface. For example, when $\tau = 0$, $p_1(0) = 0$, $p_2(0) =$

-0.00025. In order to compare the experimental results of Refs.[13–15] with our theoretical analysis, the choices of parameters are similar to those used in experiments. For instance, the internal radius of the circular cylindrical container is 7.5cm, the depth of fluid is 0.5–2.0cm, the externally excited amplitude and frequency of the vessel are in a range of 0.114–0.414mm and 10–60Hz respectively.

When $M_1=-5$, $\sigma=5$, solving Eqs.(2) and (3) yields the evolution of amplitude $p_1(\tau)$ with the slowly varying time τ for different values of M_2 , as shown in

Fig.2 (the time t in Fig.2 is equal to the time τ in Eqs.(2) and (3)). It can be seen from Fig.2 that when the excitation parameter M_2 increases, the amplitude $p_1(\tau)$ changes with time from a quasi-periodical amplitude to a modulated one, which finally results in the formation of a sort of high frequency periodical motion. However, if the parameter M_2 increases further, (for example, when M_2 is greater than 7) the surface waves will be destabilized and their amplitudes trend to be infinite. From the investigations in Refs.[16–19], the parameter M_2 is related to the forced frequency.

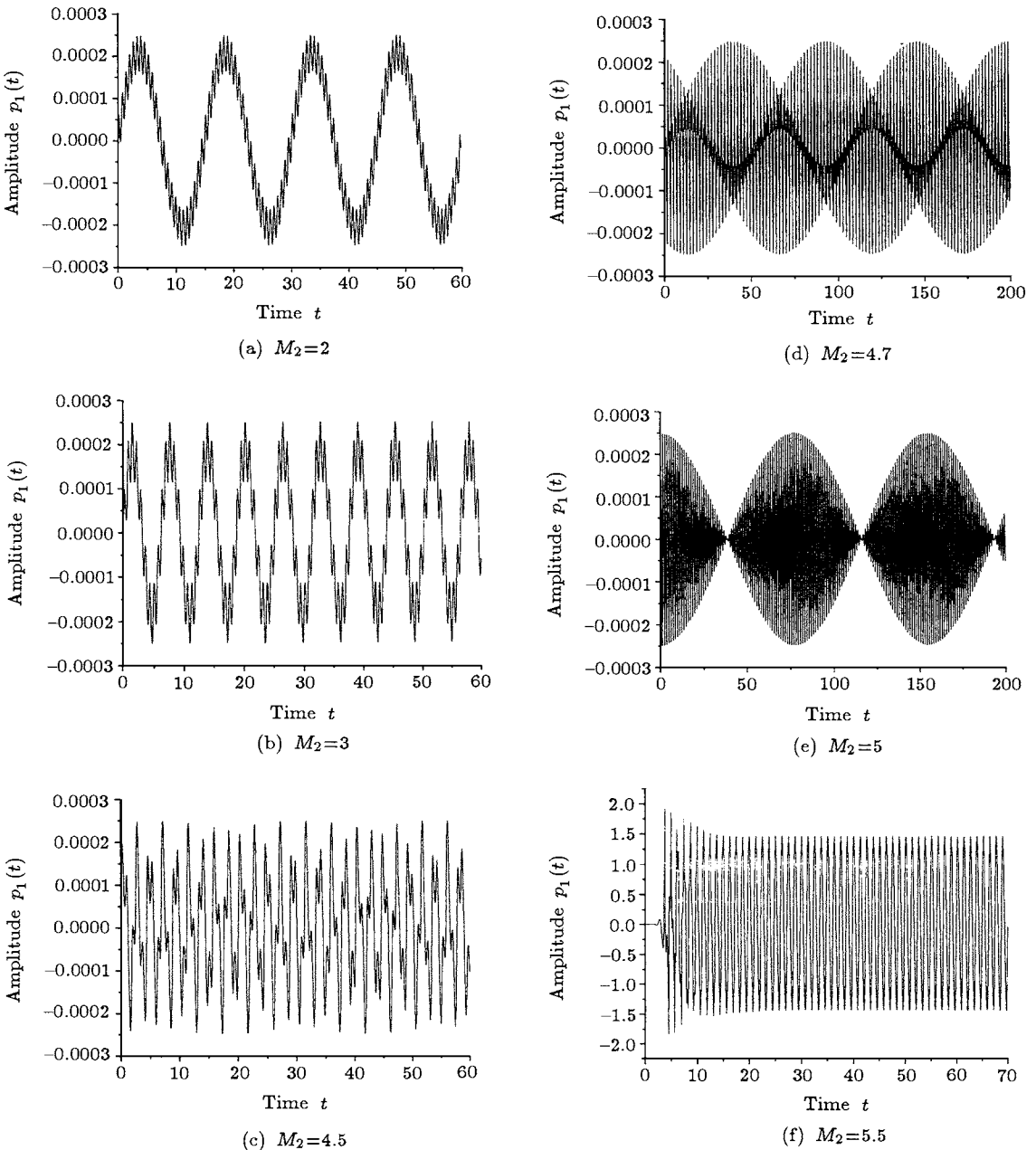


Fig.2. Evolution of amplitude $p_1(\tau)$ with time τ from equations (2) and (3). ($M_1=-5$, $\sigma=5$, initial conditions are $p_1(0) = 0$ and $p_2(0) = -0.00025$).

A clear physical explanation of these numerical results is that with the increase of the forced frequency M_2 , the parameter ε may become so large that the assumption that it is much less than unity cannot hold true, thereby the amplitude equations (2) and (3) may not be used to describe the motion of surface wave any more.

The phase-plane trajectories corresponding to

Fig.2, which are determined by amplitudes $p_1(\tau)$ and $p_2(\tau)$ from Eqs.(2) and (3), are displayed in Fig.3. From Fig.3, it is seen that the phase-plane trajectories are shaped into closed spiral lines, ringed regions, circular regions and limit cycles with periodical solution. Similarly, quasi-periodical surface waves, modulated amplitude and high frequency periodical solution can be found in Fig.3.

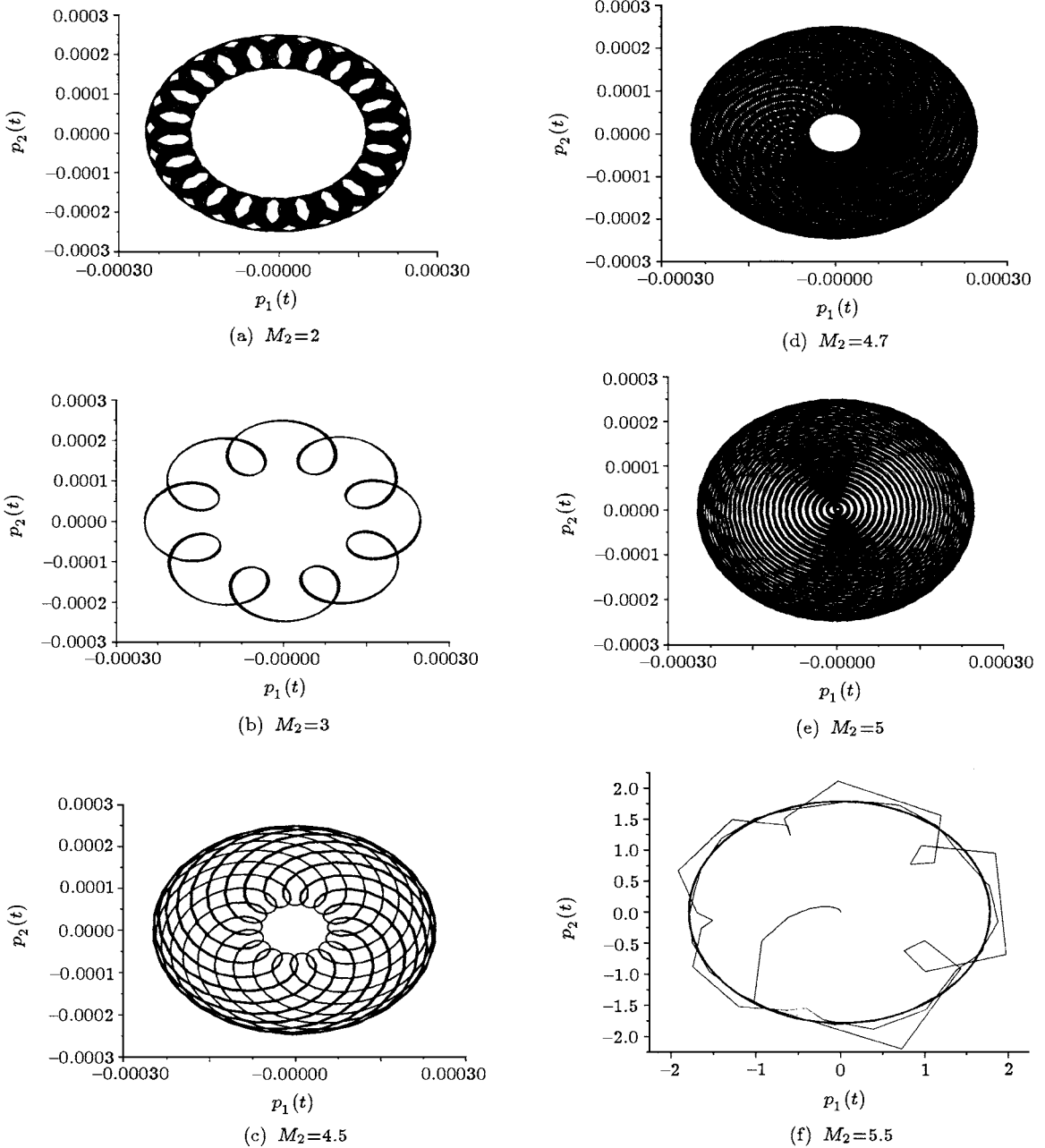
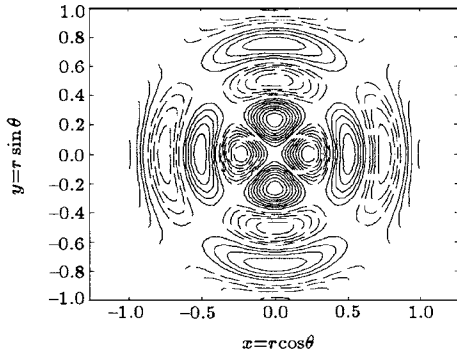


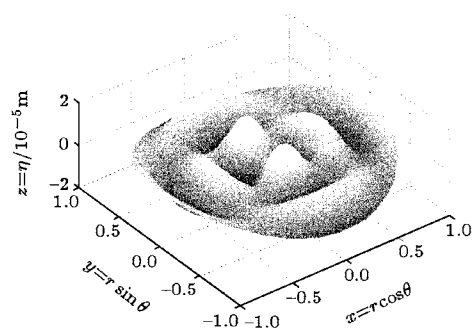
Fig.3. Phase-plane trajectories determined by amplitudes $p_1(\tau)$ and $p_2(\tau)$.

4. The characteristics of the surface waves

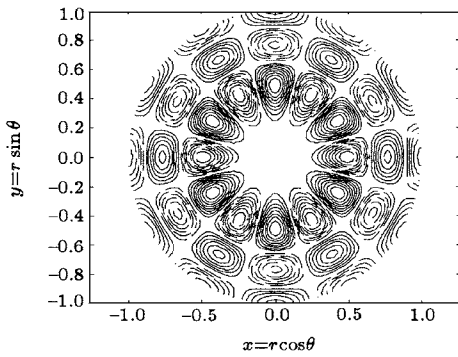
If the forced amplitude is fixed, different forced frequencies will produce different surface wave modes.



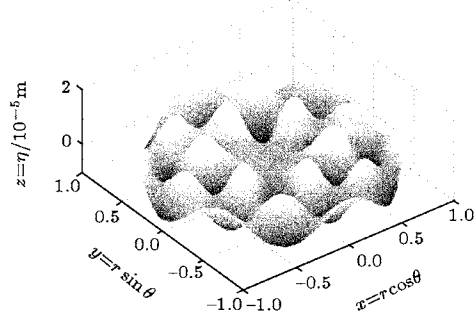
(a₁) Contour of (2, 4) mode ($f=12.85\text{Hz}$).



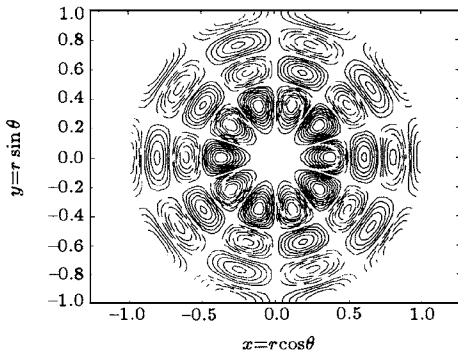
(a₂) Three-dimensional surface figure of (2, 4) mode.



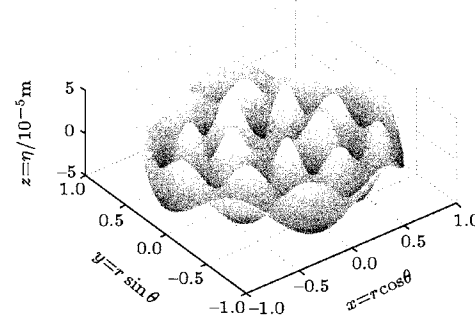
(b₁) Contour of (6, 3) mode ($f=13.90\text{Hz}$).



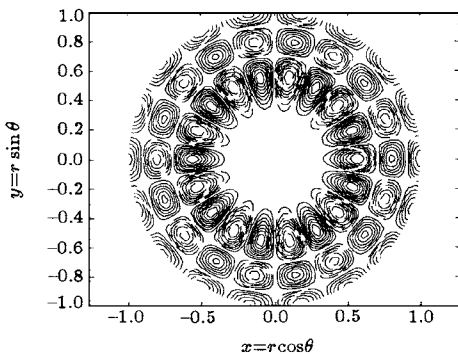
(b₂) Three-dimensional surface figure of (6, 3) mode.



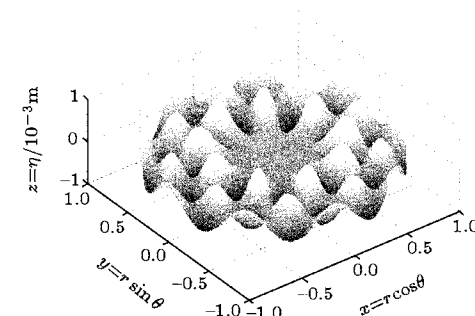
(c₁) Contour of (5, 4) mode ($f=14.95\text{Hz}$).



(c₂) Three-dimensional surface figure of (5, 4) mode.



(d₁) Contour of (9, 3) mode ($f=15.73\text{Hz}$).



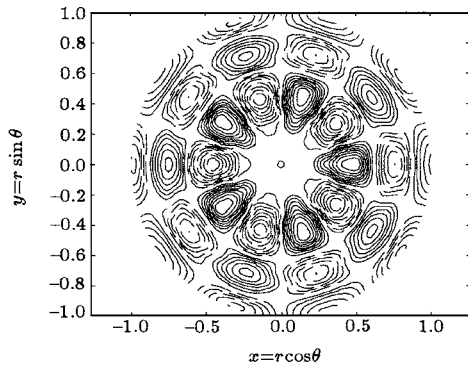
(d₂) Three-dimensional surface figure of (9, 3) mode.

Fig.4. Contours (left) and three-dimensional surface figures (right) of the free surface displacement at different forced frequencies (the forcing amplitude $A=11.4\mu\text{m}$).

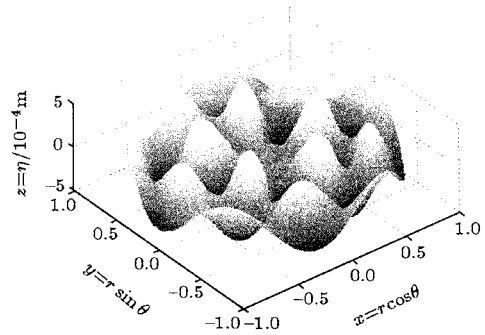
For example, the forced amplitude is fixed at $11.4\mu\text{m}$ and forced frequencies f are 12.85, 13.90, 14.95, 15.73 and 20.56Hz, the contours and corresponding three-dimensional surface figures of the free surface displacements, which are determined by Eq.(4), are plotted in Fig.4 at the fixed time $t = 215.9\text{s}$. In Fig.4, the solid and dashed lines denote the positions of free surface above and below the equilibrium surface, respectively. The parametrical couple of (m, n) in Fig.4 and the following indicate that there are m wave-crests in circumferential direction and n zero points in radical di-

rection.

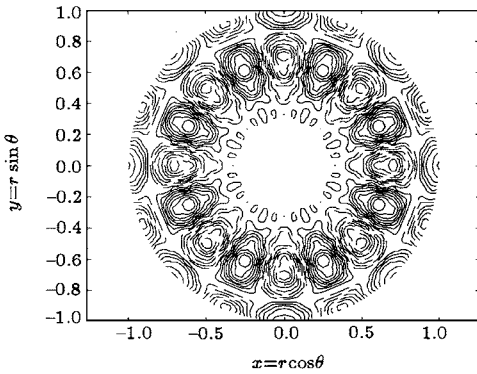
It can be shown that the shapes of the excited modes of the surface waves become more and more complex with increasing the forced frequency. Most of the modes of the surface waves have not been reported and only a few modes were observed in the experiments of Refs.[13–15]. In his experiments, the side-wall was kept stationary and only the bottom of the vessel oscillated vertically. The viscous effect was large in his experiments as compared to that in the original work by Faraday.



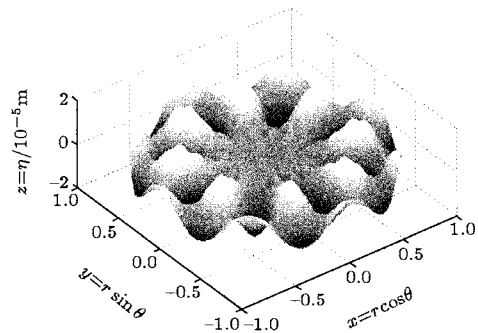
(a₁) Contour of (5, 3) mode ($f=13.3\text{Hz}$).



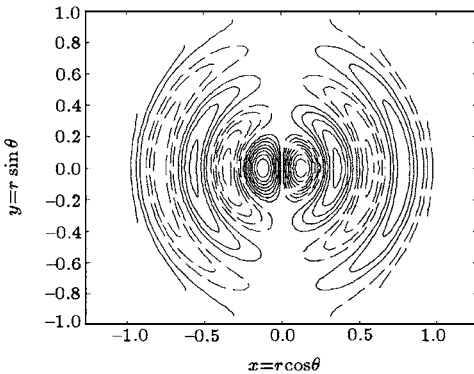
(a₂) Three-dimensional surface figure of (5, 3) mode.



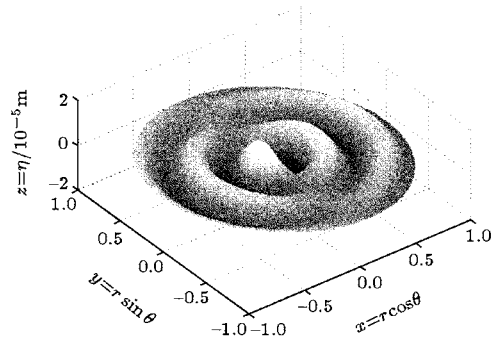
(b₁) Contour of (8, 2) mode ($f=13.4\text{Hz}$).



(b₂) Three-dimensional surface figure of (8, 2) mode.



(c₁) Contour of (1, 5) mode ($f=13.7\text{Hz}$).



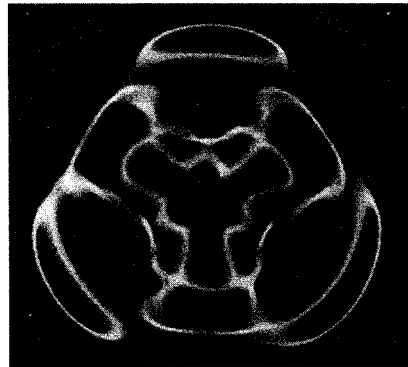
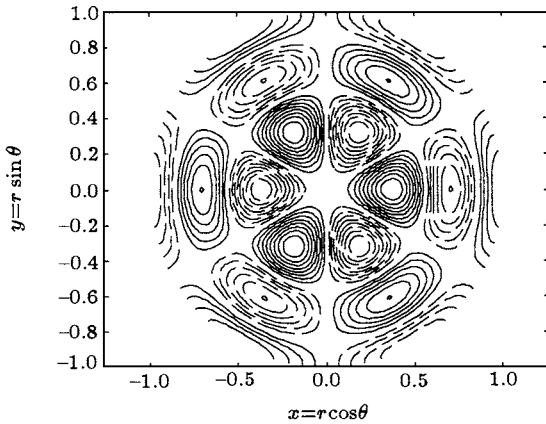
(c₂) Three-dimensional surface figure of (1, 5) mode.

Fig.5. Selection of surface wave modes caused by a small change of forced frequency. Contours (left) and three-dimensional surface figures (right) of the free surface displacement (the forcing amplitude $A=11.4\mu\text{m}$).

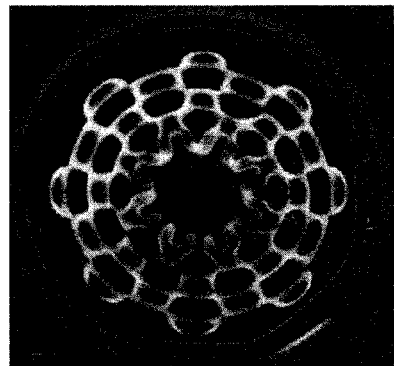
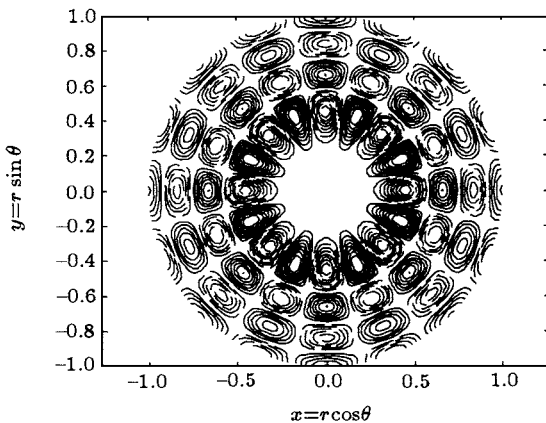
We find that the mode choices of the surface waves are very sensitive to a small change of the forced frequency when the forced frequency is higher. This conclusion is illustrated in Fig.5 at the forced frequencies of 13.3, 13.4, and 13.7Hz respectively. The contours and three-dimensional surface of the free surface displacement are displayed in Fig.5 with a forced amplitude $A=11.4\mu\text{m}$. The meanings of solid lines and dashed lines in Fig.5 are similar to those in Fig.4.

5. The comparison with experimental measurements

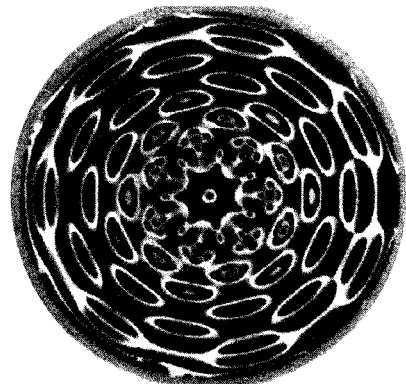
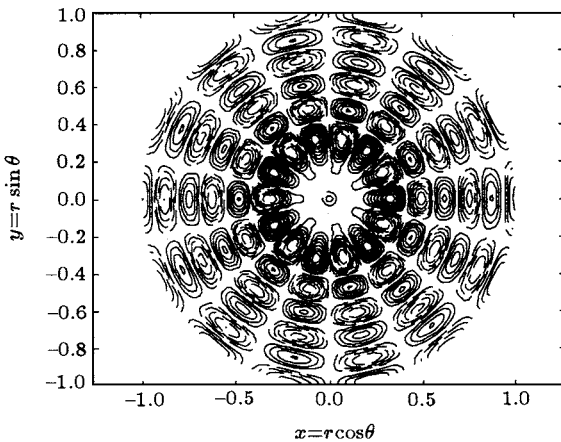
A comparison can be made between the theoretical and experimental contours at different forcing frequencies, as shown in Fig.6. Although the forcing frequencies are smaller than those in the experiments of Refs.[13-15], as predicted by our theory, these experimental flowing patterns conform with the theoretical ones.



(a₁) Theoretical contour of (3, 3) mode ($f=11.68\text{Hz}$). (a₂) Experimental contour of (3, 3) mode ($f=20\text{Hz}$).



(b₁) Theoretical contour of (8, 4) mode ($f=16.71\text{Hz}$). (b₂) Experimental contour of (8, 4) mode ($f=50\text{Hz}$).



(c₁) Theoretical contour of (7, 6) mode ($f=18.741\text{Hz}$). (c₂) Experimental contour of (7, 6) mode ($f=52\text{Hz}$).

Fig.6. Comparison of theoretical contours of surface wave mode with those in experiment (depth of fluid $h=1.0\text{cm}$, radius of the vessel $R=7.5\text{cm}$, the forcing amplitude $A=11.4\mu\text{m}$).

To some extent, the discrepancy is possible due to the following two reasons. Firstly, the scales of our computational modelling are small (for example, the radius of container is 7.5cm, and forced amplitude is just of the order of μm), so the influence of the surface tension on mode selection plays a substantial role (Jian^[20] (2003) has proved that the theoretical forced frequencies are 12.6Hz, 21.1Hz and 26.0Hz respectively in Figs.6(a₁), 6(b₁), and 6(c₁)). Moreover, with the increase of the forced frequency, the effect of surface tension becomes more important. Secondly, since our modelling is established in inviscid fluids, it is difficult to make a quantitative comparison of our present theoretical analysis with the experimental measurements due to the presence of some parasitic dissipative mechanisms that are beyond the idealized theoretical assumptions, such as the damping in the viscous boundary layers along the sidewalls (Refs.[19,20] have considered the mode selection in weakly viscous fluids, and the theoretical forced frequencies are modified to 19.1Hz, 22.5Hz and 26.7Hz respectively in Figs.6(a₁), 6(b₁), and 6(c₁) with the effect of both surface tension and weak viscosity), and dissipation resulting from both the moving contact line of the meniscus (Ref.[10] has identified that the damping from the moving contact line makes a considerable contribution to the dissipation, which accounts for 10%–20% of the bulk dissipation) and the surface viscosity of surfactant films.

The influence of the surface tension and viscos-

ity in the mode selection will be discussed in other papers, and the deviation between theoretical calculations and experimental measurements will be further improved.

6. Conclusions

From the above analyses, we obtain the following results:

1. The nonlinear amplitude Eqs.(2) and (3) and free surface displacement Eq.(4) can be used to correctly describe the surface wave motion in a vertically excited vessel.
2. The slowly varying amplitude $p(\tau)$ changes from a quasi-periodical amplitude to a modulated one and finally appears a high frequency periodical motion with the increase of the forced frequency.
3. The mode selection of the surface waves is very sensitive to a small change of the forced frequency when the forced frequency is higher.
4. The structure of the surface waves become complex with the increase of the forcing frequency. Many unreported surface wave modes have been found by numerical computation and these can be used to explain many patterns appearing in the experiment.

Acknowledgement

The authors are grateful to Professor Zhou Xi-anchu for discussion on the mathematical treatment, and Dr Bai Wei for assistance in the numerical work.

References

- [1] Faraday M 1831 *Phil. Trans. R. Soc. Lond.* **121** 319
- [2] Benjamin T B and Ursell F 1954 *Proc. R. Soc. Lond.* **255** 505
- [3] Skalak R and Yarymovich M 1962 *Proc. 4th US Natl Congr. Appl. Mech.* 1411
- [4] Ockendon J R and Ockendon H 1973 *J. Fluid Mech.* **59** 397
- [5] Miles J W 1984a *J. Fluid Mech.* **146** 285
- [6] Miles J W 1993 *J. Fluid Mech.* **248** 671
- [7] Miles J W and Henderson D 1990 *Ann. Rev. Fluid Mech.* **22** 143
- [8] Kumar K and Tuckerman L 1994 *J. Fluid Mech.* **279** 49
- [9] Cerda E A and Tirapegui E L 1998 *J. Fluid Mech.* **368** 195
- [10] Christiansen B *et al* 1995 *J. Fluid Mech.* **291**323
- [11] Ciliberto S and Gollub J P 1985 *J. Fluid Mech.* **158** 381
- [12] Gollub J P and Meyer C W 1983 *Physica D* **6** 337
- [13] E X Q and Gao Y X 1996 *Commun. Nonlinear Sci. Numer. Simul.* **1** 1
- [14] E X Q and Gao Y X 1996 *Proc. 4th Asian Symposium on Visualization Beijing* p653
- [15] Gao Y X and E X Q 1998 *Exp. Mech.* **13** 326 (in Chinese)
- [16] Jian Y J *et al* 2003 *Appl. Math. Mech.* **24** 1194
- [17] Jian Y J and E X Q 2003 *J. Hydrodynam.* **18** 135 (in Chinese)
- [18] Jian Y J and E X Q 2004 *Adv. Mech.* **34**(1) 61 (in Chinese)
- [19] Jian Y J and E X Q 2004 *Chin. Phys.* **13** 1191
- [20] Jian Y J 2003 *PhD Thesis* (Institute of Mechanics, Chinese Academy of Sciences)